

## Study on Coaxially Electrospinning Nanofibers for Deep Partial-thickness Burns

LIU Xiaoyan<sup>1</sup>, ZHU Siqing<sup>1,2</sup>, ZHANG Lihua<sup>1,3</sup>, SUN Jinjie<sup>4</sup>, DU Lina<sup>1,2,3\*</sup>, JIN Yiguang<sup>1,2</sup> (1. Department of Pharmaceutical Sciences, Beijing Institute of Radiation Medicine, Beijing 100850, China; 2. Anhui Medical University, Hefei 230001, China; 3. Shandong University of Traditional Chinese Medicine, Jinan 250355, China; 4. Air Force Medical Center, PLA, Beijing 100142, China)

**ABSTRACT: OBJECTIVE** To observe the effect of alginate/polyvinyl alcohol (PVA)/chitosan coaxial nanofibers on healing of deep partial-thickness burn in rats. **METHODS** Coaxial nanofibers composed of sodium alginate/PVA/chitosan were prepared with coaxial electrospinning technology, Scanning electron microscopy, transmission electron microscopy and X-ray diffraction techniques were used to characterize morphology and composition. Water absorption and antibacterial ability *in vitro* were evaluated. Sprague-Dawley rats with deep partial-thickness burns were randomly divided into 2 groups, the model group without treatment and the coaxial nanofiber treatment group. Wound healing and pathological slides were observed. The expression of vascular endothelial growth factor (VEGF), differentiation cluster 31 (CD31) and proliferating cell nuclear antigen (PCNA) were determined by immunohistochemical staining. Tumor necrosis factor- $\alpha$  (TNF- $\alpha$ ) and interleukin-6 (IL-6) were determined by ELISA. **RESULTS** Obvious core-shell structure of coaxial nanofibers were observed. Coaxial nanofibers were highly absorbent and had good effect in bacterial inhibition. Low infiltration of inflammatory cells and much collagen formation in the wound tissue were observed by H.E. staining and Masson staining on the 5th, 14th and 21st day after burn. Compared with the model group, coaxial nanofiber group shortened wound healing time, increased wound healing rate ( $P < 0.01$ ) with less inflammatory cell infiltration and promoted collagen production. Coaxial nanofibers could effectively increase expression of VEGF, CD 31, PCNA, and decrease TNF- $\alpha$  and IL-6 levels ( $P < 0.01$ ). **CONCLUSION** Sodium alginate/PVA/chitosan coaxial nanofibers can effectively promote the healing of deep burn wounds by promoting the proliferation of wound cells and synthesis of collagen. It can be used as a novel wound dressing for treatment of deep partial-thickness burns.

**KEYWORDS:** alginate; burn; chitosan; coaxial nanofibers; electrospinning; wound healing

## 治疗深 II 度烧伤的同轴静电纺丝纳米纤维的研究

刘晓妍<sup>1</sup>, 朱思庆<sup>1,2</sup>, 张丽花<sup>1,3</sup>, 孙金杰<sup>4</sup>, 杜丽娜<sup>1,2,3\*</sup>, 金义光<sup>1,2</sup> (1. 军事科学院军事医学研究院辐射医学研究所抗辐射药物研究室, 北京 100850; 2. 安徽医科大学, 合肥 230001; 3. 山东中医药大学, 济南 250355; 4. 空军特色医学中心, 北京 100142)

**摘要: 目的** 研究海藻酸钠/聚乙烯醇(polyvinyl alcohol, PVA)/壳聚糖同轴纳米纤维对大鼠深 II 度烧伤模型的促愈合作用。**方法** 采用同轴静电纺丝技术制备由海藻酸钠/PVA/壳聚糖组成的同轴纳米纤维, 扫描电镜、透射电镜、X 射线衍射技术进行性质表征, 体外实验考察其吸水性、抑菌性能。建立 SD 大鼠深 II 度烧伤创面模型, 随机分成模型组和同轴纳米纤维组。观察大鼠创面愈合情况、病理学改变, 用免疫组化法检测创面血管内皮生长因子(vascular endothelial growth factor, VEGF)、分化簇 31(differentiation cluster 31, CD31)和增殖细胞核抗原(proliferating cell nuclear antigen, PCNA)的表达, ELISA 测定肿瘤坏死因子(tumor necrosis factor- $\alpha$ , TNF- $\alpha$ )和白介素-6(interleukin-6, IL-6)水平。**结果** 同轴纳米纤维具有明显的核壳结构, 吸水性好, 体外抑菌作用明显。在治疗后 5, 14, 21 d 观察到炎性细胞浸润减少、胶原蛋白生成增加。与模型组比较, 同轴纳米纤维组伤口愈合时间缩短, 伤口愈合率高( $P < 0.01$ ), 炎性细胞浸润减少, 胶原蛋白生成增加。同轴纳米纤维能有效促进 VEGF、CD31、PCNA 表达, 降低炎症因子 TNF- $\alpha$  和 IL-6 水平( $P < 0.01$ )。**结论** 通过促进创面细胞增殖及胶原的合成, 海藻酸钠/PVA/壳聚糖同轴纳米纤维能有效促进深 II 度烧伤创口愈合, 可作为一种新型治疗深 II 度烧伤的外用敷料。

**关键词:** 海藻酸钠; 烧伤; 壳聚糖; 同轴纳米纤维; 静电纺丝技术; 伤口愈合

中图分类号: R285.5 文献标志码: A 文章编号: 1007-7693(2019)07-0773-08

DOI: 10.13748/j.cnki.issn1007-7693.2019.07.001

引用本文: 刘晓妍, 朱思庆, 张丽花, 等. 治疗深 II 度烧伤的同轴静电纺丝纳米纤维的研究[J]. 中国现代应用药学, 2019, 36(7): 773-780.

基金项目: 国家自然科学基金项目(81441095)

作者简介: 刘晓妍, 女, 硕士生 Tel: (010)66930216 E-mail: liuxiaoyan9645@126.com \*通信作者: 杜丽娜, 女, 博士, 副研究员 Tel: (010)66930216 E-mail: dulina@188.com

## Introduction

Burns are the severe diseases with enormous cost of treatment, mortality and considerable morbidity. Millions of patients suffer from burns, where deep partial-thickness burns are common involving destruction of the entire epidermis and a substantial part of the dermis. Healing speed and extension of burned tissues predominantly depend on the depth of injured skins. Superficial burns can re-epithelialize very fast with minimal scars, whereas, deep partial-thickness burns may take a few weeks to heal and tend to form severe scars<sup>[1]</sup>. Currently, treatment challenges of deep partial-thickness burns are how to protect wounds from bacterial infection, absorb the exudates from burn wounds, and hinder the formation of scars. Previously, asiaticoside-loaded coaxially electrospinning nanofibers showed good treatment efficacy in deep partial-thickness burns<sup>[2]</sup>. However, it's not clear if the blank electrospinning nanofibers have the same or better effect.

A typical electrospinning instrument works with a high voltage source that adds charges to a polymer solution or melt. The charged polymer solution or melt is accelerated toward a collector of opposite polarity under a high-voltage electrostatic field due to the strong electrostatic attraction. At the same time, intra-liquid strong electrostatic repulsions happen. A fiber jet is ejected from the leading-edged Taylor cone as the electric field strength exceeds the surface tension of the liquid. The fiber jet travels through the atmosphere to allow solvent evaporating, leading to the deposition of solid polymer fibers on the collector<sup>[3]</sup>. Fiber produced with this process has diameters on the order of a few micrometers down to the tens of nanometers<sup>[4]</sup>. A spinner composed of two coaxial capillaries was developed for simultaneously electrospinning of two different polymer solutions into core-shell structured nanofibers<sup>[5]</sup>. The coaxially electrospinning technique can make non-electrospun polymers being electrospun as the core layer.

Here a novel coaxially electrospinning nanofiber with core-shell structure<sup>[6]</sup> composed of chitosan-core/sodium alginate-shell was prepared to cure burns. Chitosan is difficult for electrospinning if alone used<sup>[7-8]</sup>. However, this work make it electrospun in this coaxial nanofiber. Therefore, the coaxial nanofibers could take a combinatorial

function of chitosan and alginate, including strong water adsorption and antimicrobial ability, which would benefit wound healing. The *in vitro* and *in vivo* properties of the coaxial nanofibers were explored.

## 1 Experimental

### 1.1 Materials

Sodium alginate (Lot# S20527, viscosity of 200±20 mPa·S) and chitosan (Lot# YZ 20081126, degree of deacetylation of 89%, MW of 60 kDa) were purchased from Sinopharm Chemical Reagent Co., Ltd. (Beijing, China). Polyvinyl alcohol (PVA, Lot# 20150429, MW of 77 000 kDa) was purchased from Beijing Yili Fine Chemicals Co., Ltd., China. Organic solvents were of analytical grade. The other chemicals were of reagent grade. The ELISA kits (Lot# R180906-002a, Lot# R180116-102a) for determination of interleukin-6 (IL-6) and tumor necrosis factor- $\alpha$  (TNF- $\alpha$ ) were purchased from Neobioscience Technology Co., Ltd., Wuhan, China.

### 1.2 Animals

Healthy male Sprague-Dawley rats (weight of 180–200 g) were obtained from the Vital River Laboratory Animal Technology Co., Ltd. (Beijing, China). All the animals had free access to standard diet and water. The animals were sacrificed to obtain tissues. Principles in good laboratory animal care were followed and people taking part in the animal experiments owned the licenses for animal surgery. Animal experiments were conducted in accordance with the Guidelines for the Care and Use of Laboratory Animals in the institute, and the National Institute of Health (NIH) guide for the care and use of laboratory animals. License number of laboratory animal was SCXK (Jing) 2016-0006.

### 1.3 Electrospinning

A mixture of sodium alginate/PVA was added into the 10% acetic acid solution and agitated for 5 h at 90 °C to obtain the shell-forming solution. The core-forming solution was prepared after chitosan was dissolved in the 2% acetic acid solution. Coaxial nanofibers were prepared with an electrospinning equipment (SS-2535H, Beijing Ucalery Technology Development Co., Ltd., China) installed with the coaxial injectors. During electrospinning, a voltage of 23 kV was applied between the needle and the collector. The acceptance distance was 15 cm and the pushing rate of the shell and core solutions was 0.8,

0.2 mL·h<sup>-1</sup>, respectively. The alginate/PVA nanofibers were also prepared as above with 7% PVA and 0.8% alginate in the electrospun solution and the pushing rate of 0.8 mL·h<sup>-1</sup>. So was the chitosan/PVA nanofiber with 7% PVA and 3% chitosan in the solution.

#### 1.4 Characterization of nanofibers

The morphologies of nanofibers were observed on a scanning electron microscope (SEM, 5 kV, S-4800, Hitachi, Japan) and a transmission electron microscope (TEM, 80 kV, H-7650, Hitachi, Japan). The diameters of nanofibers were analyzed with the image analysis software (Image J, NIH, USA). The average diameter of nanofibers was statistically calculated with at least 100 randomly selected fibers.

The coaxial nanofibers and the physical mixture of alginate/PVA/chitosan were characterized by the X-ray diffraction (XRD, D8-advance, Bruker, Germany) with diffraction angle from 5° to 45° for their structural properties and the Fourier transform infrared spectrum (FTIR, Nicolet 6700, Thermo Fisher Co., USA).

#### 1.5 Water absorption of nanofibers

A piece of films (2 cm×2 cm) containing nanofibers was weighed ( $W_0$ ). It was immersed into deionized water (5 mL). At the predetermined time points of 0.5, 1, 2, 4, 6, 8, 10, 12, 48 h, the sample was lifted off followed by removal of water with a filter paper. The hydrated nanofibers were weighed ( $W_1$ ). Water absorption capacities of the following three types of nanofibers were calculated as Eq. (1)<sup>[9-10]</sup>, including the coaxial nanofibers of alginate/PVA/chitosan, the nanofibers of alginate/PVA, and the nanofibers of chitosan/PVA.

$$\text{Water absorption}=(W_1-W_0)/W_0\times 100\% \quad (1)$$

#### 1.6 Antibacterial assessment of nanofibers<sup>[11]</sup>

A Gram-positive bacterium, *Staphylococcus aureus* (ATCC 25923) and a Gram-negative bacterium, *Pseudomonas aeruginosa* (ATCC 27853) were used for antibacterial assessment. *S. aureus* and *P. aeruginosa* were precultured in the Luria-Bertani Broth (LB) overnight in a rotary shaker at 37 °C. The concentration of bacterial suspension was determined by the counting method with a blood cell counting plate. An aliquot (100 μL) of diluted bacterial suspensions (1 010 CFU·mL<sup>-1</sup>) was seeded on the LB agar media using a spread plate.

Antibacterial assessment was tested with the disk diffusion method<sup>[12-13]</sup>. Both of the alginate/PVA/chitosan and the alginate/PVA nanofibers were cut to 8 mm-in-diameter discs that were then put on the surfaces of the petri dishes. The plates were incubated at 37 °C for 24 h followed by determination of inhibition zones.

#### 1.7 Pharmacodynamics study

##### 1.7.1 Animal model of deep partial-thickness burns

Fourteen rats were anesthetized with the 10% chloral hydrate solution and the dose of 4 mL·kg<sup>-1</sup>. Deep partial-thickness burn wounds were established with a specially designed electric heating instrument (YLS-5Q, Bio-will Co., Ltd., Shanghai, China) that was able to control the heating cylinder temperature and pressing pressure. The wounds were confirmed after staining with hematoxylin and eosin (H&E).

##### 1.7.2 Treatment protocols of wounds

Fourteen burned rats were randomly divided into two groups: the model group without treatment, the coaxial nanofiber group with the alginate/PVA/chitosan coaxial nanofibers (30 mg) being covered on the wounds once every day. On days 1, 5, 10, 14 and 21 following burning, the wounds were photographed and the wound area was analyzed with an image analysis software (Image Pro Plus 6.0, Media Cybernetics, USA). The percentage of wound healing was defined as Eq. 2.

$$\text{Wound healing}=(A_1-A_n)/A_1\times 100\% \quad (2)$$

Where  $A_n$  was the wound area on a given day after burns, and  $A_1$  was the wound area on the first day.

##### 1.7.3 Pathological investigation

The full-thickness wound skins were taken on days 5, 14 and 21 following burning. The tissue samples were fixed in the 10% formaldehyde solutions, embedded in paraffin and cut into 5 μm thick sections. The sections were stained with H&E and Masson's trichrome. The slides were observed on an optical microscope (BDS200-FL, Chongqing Optec Instrument Co., Ltd., China).

##### 1.7.4 Immunohistochemical investigation

Expression of vascular endothelial growth factor (VEGF), cluster of differentiation 31 (CD31), and proliferating cell nuclear antigen (PCNA) in the wounded tissues were determined with immunohistochemical staining. The sections of

wounds were initially embedded in paraffin, and then deparaffinized, rehydrated, and microwave-heated for 15 min in the EDTA antigen retrieval solution (pH 8.0) for antigen retrieval. Then, a 3% hydrogen peroxide solution was applied to block the endogenous peroxidase activity. Furthermore, the tissues were blocked with bovine serum albumin (BSA) for 15 min. The primary antibody of CD31/VEGF/PCNA (Goodbio, Wuhan, China) diluted with a 3% BSA solution was added to the above tissues and incubated overnight at 4 °C. The sections were washed with PBS for three times and 5 min once. The secondary antibody of primary antibody was added and incubated for 30 min at room temperature followed by interval PBS washing. The sections were immersed for 5 min in the coloring substrate 3,3'-diaminobenzidine (DAB, 0.4 mg·mL<sup>-1</sup>, DAKO, USA) containing 0.003% hydrogen peroxide, rinsed with water, counterstained with hematoxylin, dehydrated, and coverslipped. The sections were further observed on a microscope.

### 1.7.5 Detection of inflammatory factors

The full-thickness wound skins of about 0.2 g were taken out on days 5, 14 and 21 after burning. They were smashed into homogenates in an ice-cold bath with a high-speed tissue homogenizer (IKA T10 BS25, Staufen, Germany). The homogenates were centrifuged at 3 700 g. A 2 mL aliquot of supernatants was withdrawn for the ELISA determination of TNF- $\alpha$  and IL-6 according to the instructions.

### 1.8 Statistical analysis

The data were treated statistically with the SPSS software (Version 16.0, SPSS Inc., Chicago, IL, USA) and data were expressed as  $\bar{x} \pm s$ . LSD test was employed to identify significant differences ( $P < 0.05$ , or  $P < 0.01$ ) between data sets.

## 2 Results

### 2.1 Characteristics of coaxially electrospinning nanofibers

The final formulation of coaxially electrospinning nanofibers consisted of 7% PVA and 0.8% sodium alginate in the shell-forming solution and 3% chitosan in the core-forming solution. The coaxial nanofibers showed smooth surfaces, and uniform diameter distribution (Fig. 1). However, SEM images could not reveal the inner structures of coaxial nanofibers. In this study, the typical core-shell structure of coaxial nanofibers was

observed with the TEM (Fig. 2).

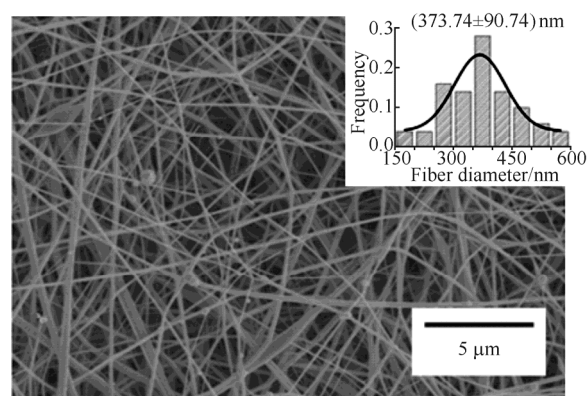


**Fig. 1** SEM image of characteristics and diameter distribution of alginate/PVA/chitosan coaxial nanofibers

**图 1** 海藻酸钠/PVA/壳聚糖同轴纳米纤维表征 SEM 照片和直径分布

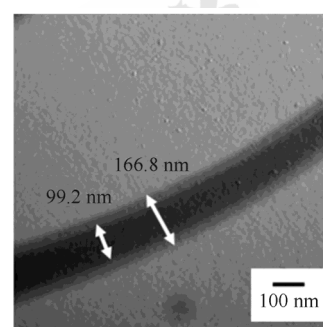


**Fig. 2** TEM image of the coaxial nanofiber with the obvious core-shell structure

**图 2** 有明显核-壳结构的同轴纳米纤维的 TEM 照片

For the physical mixture did not interact with each other, the XRD graphs showed the crystal region with obvious diffraction peaks at  $2\theta = 12^\circ$ ,  $19.5^\circ$ ,  $23^\circ$ ,  $40.5^\circ$ , respectively. And the diffraction intensity at  $2\theta = 19.5^\circ$  was the highest. The diffraction peaks of the coaxial nanofibers at  $2\theta = 12^\circ$  and  $19.5^\circ$  became very weak compared to that of the physical mixture. It demonstrated that the composition of the coaxial nanofibers was no longer a simple physical mixture. The crystal structure changed during the electrospinning process (Fig. 3A).

As for physical mixture of FTIR, typical absorbance peaks appeared at  $3\ 405\ \text{cm}^{-1}$  (flexible vibration of O-H and N-H),  $2\ 938\ \text{cm}^{-1}$  (flexible vibration of C-H),  $1\ 654\ \text{cm}^{-1}$  (carbonyl group),  $1\ 088\ \text{cm}^{-1}$  (flexible vibration of C-O and bending vibration of O-H),  $853\ \text{cm}^{-1}$  ( $\beta$ -glucoside bonds of chitosan), respectively. After nanofibers were electrospun, the typical absorbance peak at  $3\ 423\ \text{cm}^{-1}$  became sharper and stronger. It

suggested that hydrogen bond might form between hydroxy and amino groups. Hydrogen bond might decrease the impedance of amino groups on electrospinning and favorable for electrospinning. Crystal structure of chitosan weakened due to the peak at  $1\ 092\ \text{cm}^{-1}$  decreased (Fig. 3B).

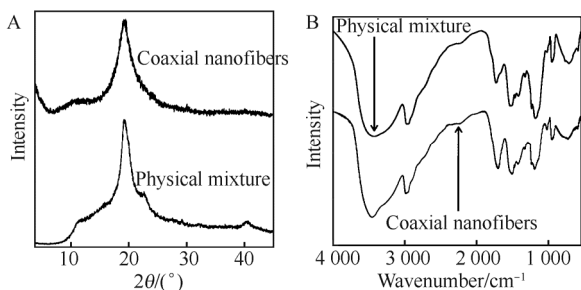


**Fig. 3** XRD graphs(A) and FTIR spectra(B) of the coaxial nanofibers and physical mixtures of alginate/PVA/chitosan

**图 3** 海藻酸钠/PVA/壳聚糖物理混合物及其同轴纳米纤维 XRD 图(A)和 FTIR 光谱(B)

TEM images showed that the coaxial nanofiber had a uniform core-shell structure with the outer and inner layers at nanoscale. The XRD and FTIR analyses indicated the physical status and bonding interaction of the components in the physical mixture and the coaxial nanofibers. Both of the results showed the components in the coaxial nanofibers were different from those in the physical mixture. It demonstrated that interactions might appear.

## 2.2 High water absorption of coaxial nanofibers

Compared to the alginate/PVA or chitosan/PVA nanofibers, the water absorption capacity of alginate/PVA/chitosan coaxial nanofibers was significantly higher (Fig. 4). Water absorption ratio increased with prolonged time and reached nearly saturation after 12 h. The water absorption capacity of the coaxial nanofibers was a little higher than that of the alginate/PVA nanofibers (Fig. 4). According to the results of water absorption, the coaxial nanofibers and the alginate/PVA nanofibers were selected for the further exploration.

## 2.3 Antibacterial ability of coaxial nanofibers

Antibacterial ability of the alginate/PVA/chitosan coaxial nanofibers were better with the clear inhibition zones for *S. aureus* (12 mm in diameter) and *P. aeruginosa* (11 mm). In comparison, the alginate/PVA nanofibers did not show antibacterial effect (Fig. 5).

The water absorption *in vitro* and antibacterial

experiments had preliminarily reached the design aim of alginate/PVA/chitosan coaxial nanofibers, i.e., excellent absorption of wound exudates and antibacterial function.

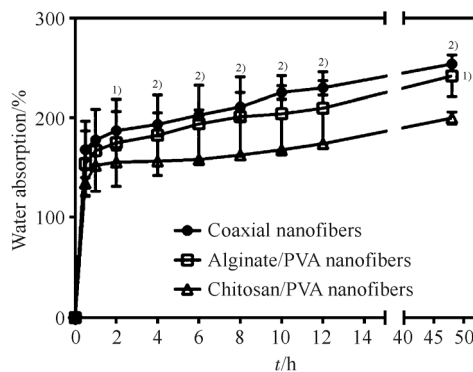


**Fig. 4** Water absorption of different nanofibers

Compared with the chitosan/PVA nanofibers, <sup>1)</sup> $P < 0.05$ , <sup>2)</sup> $P < 0.01$ .

**图 4** 不同纳米纤维吸水性

与壳聚糖/PVA 纳米纤维相比, <sup>1)</sup> $P < 0.05$ , <sup>2)</sup> $P < 0.01$ 。

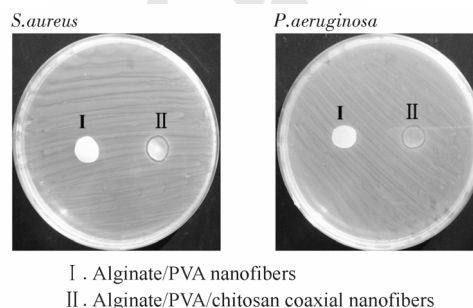


**Fig. 5** Bacterial inhibition effect of alginate/PVA and alginate/PVA/chitosan coaxial nanofibers on *S. aureus* and *P. aeruginosa*

**图 5** 海藻酸钠/PVA 和海藻酸钠/PVA/壳聚糖同轴纳米纤维对金黄色葡萄球菌和铜绿假单胞菌的抑制作用

## 2.4 Enhanced wound healing effect of coaxial nanofibers

The wounds treated with the coaxial nanofibers did not show any significant healing ratio compared to the burn wounds without any treatment within 5 days. From the 5th day, the edema of treated wound tissues began to diminish and the scabs were gradually formed (Fig. 6). New skin and hairs appeared on 10th day. On 14th day, the scabs felled off, and the new pink skin and hairs were remarkable. However, the model rats kept the large and coarse scabs at the same time. On 21st day, the treated rats had the nearly complete skins but the model rats still had the large wounds and the incomplete new skin. Wound healing was also quantified. From 5th day, the wound healing of the coaxial nanofibers was significantly higher than that without treatment

( $P < 0.01$ , Fig. 6). Therefore, the enhanced wound healing effect of the alginate/PVA/chitosan coaxial nanofibers was confirmed.

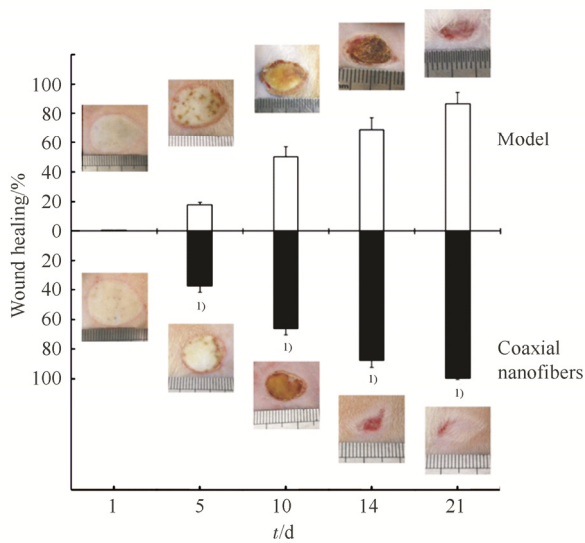


**Fig. 6** Wound healing effects of the coaxial nanofibers ( $\bar{x} \pm s$ ,  $n=6$ )

Compared with model,  $^{1)}P < 0.01$ .

**图 6** 同轴纳米纤维治疗伤口愈合的效果( $\bar{x} \pm s$ ,  $n=6$ )

与模型比较,  $^{1)}P < 0.01$ .

## 2.5 Low infiltration of inflammatory cells and much collagen formation induced by coaxial nanofibers

The burn wounds without any treatment showed the severe infiltration of inflammatory cells, and degenerated and necrotic collagens on 5th day (Fig. 7). On 14th day, the severe infiltration of inflammatory cells and the unordered skin structure still existed. However, the nanofiber-treated rats had little infiltration of inflammatory cells from 5th day, and the edema nearly disappeared and the new

vessels formed on 14th day (Fig. 7). On 21st day, collagens were produced. The epidermal structures were basically complete and similar to normal skins.

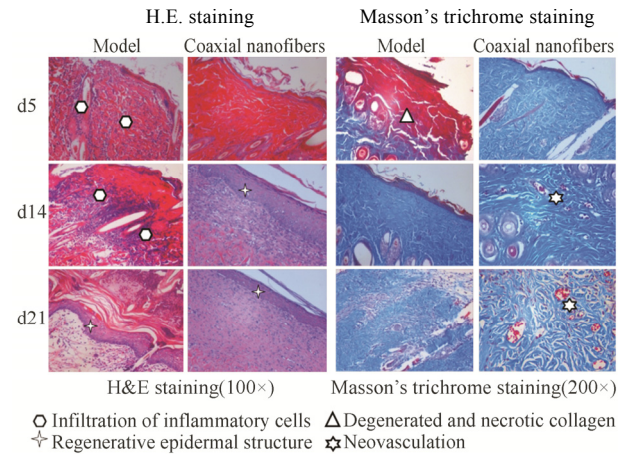


**Fig. 7** Histopathological images of burned wounds after treatment with the coaxial nanofibers

**图 7** 同轴纳米纤维治疗烧伤后的染色病理切片图

## 2.6 Effects of coaxial nanofibers on cytokines

In this study, the coaxial nanofibers remarkably up-regulated the expression of VEGF, CD31 and PCNA (Fig. 8). The coaxial nanofibers significantly decreased the levels of IL-6 and TNF- $\alpha$  after 5 d, indicating little inflammatory reactions (Fig. 9). The normal levels of IL-6 and TNF- $\alpha$  were  $(304.09 \pm 14.04) \text{pg} \cdot \text{mL}^{-1}$  and  $(516.83 \pm 20.19) \text{pg} \cdot \text{mL}^{-1}$ , respectively. After 21-day treatment, the levels of IL-6 and TNF- $\alpha$  were approximate to the normal. The coaxial nanofibers improved wound healing by decreasing infiltration of inflammatory cells and facilitating formation of collagens proved by the above results.

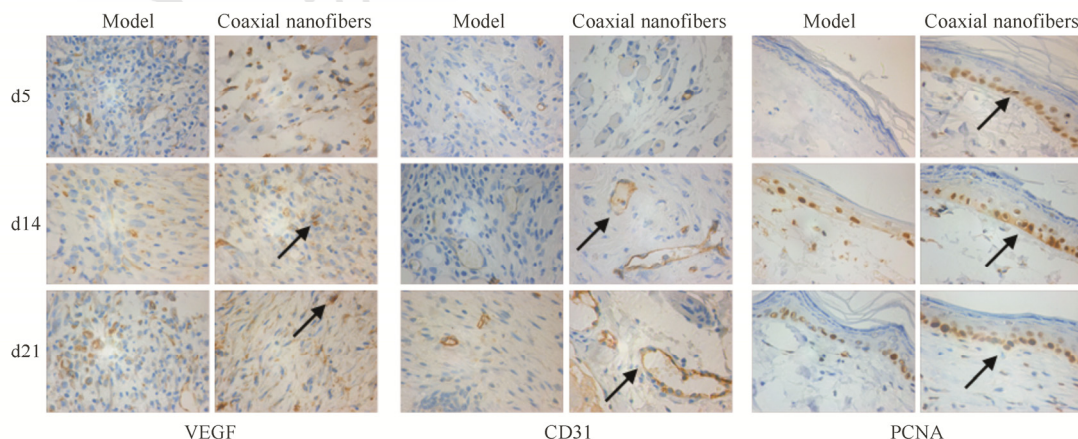


**Fig. 8** Immunohistochemical images of deep partial-thickness burns treated with the coaxial nanofibers(400 $\times$ )

Arrows indicate positive changes.

**图 8** 同轴纳米纤维治疗深 II 度烧伤后的免疫组化图(400 $\times$ )

箭头表示阳性改变。

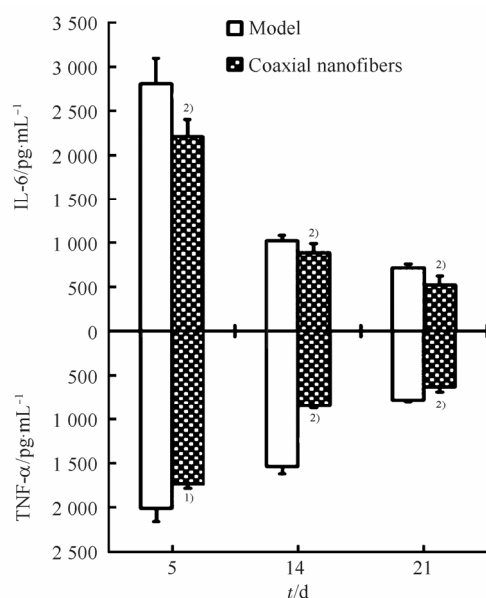


**Fig. 9** Pro-inflammatory factor level profiles after the treatment of deep partial-thickness burns with the coaxial nanofibers ( $\bar{x} \pm s$ ,  $n=6$ )

Compared with model, <sup>1)</sup> $P < 0.05$ , <sup>2)</sup> $P < 0.01$ .

**图 9** 同轴纳米纤维治疗深 II 度烧伤后的促炎因子水平 ( $\bar{x} \pm s$ ,  $n=6$ )

与模型比较, <sup>1)</sup> $P < 0.05$ , <sup>2)</sup> $P < 0.01$ 。

### 3 Discussion

One important feature of deep partial-thickness burns is with much fester. So alginate in the shell to absorb fester and chitosan in the core released in a sustained profile to inhibit bacteria growth. In addition, alginate is favorable for cells migration, adhesion and proliferation. As a result, alginate in the shell facilitated wound healing.

Viscosities and conductivities were the major factors to affect the morphologies and size of electrospinning nanofibers<sup>[14-15]</sup>. High concentrations of alginate and chitosan in the electrospinning solution resulted in large nanofiber diameters and wide distribution of the coaxial nanofibers, probably because of high viscosities and conductivities<sup>[16]</sup>. The interaction of PVA, alginate, and chitosan might affect the crystal structures of the components based on XRD results, possibly resulting from high compression in the coaxial nanofibers. FTIR spectra indicated that hydrogen bonding formed due to association of hydroxyl and amino groups in the coaxial nanofibers. Burns are characterized with a lot of exudates<sup>[17]</sup>. Therefore, higher water absorption capacity was advantageous for wound healing. On one hand, the diameter of alginate/PVA/chitosan

coaxial nanofibers with core-shell structure was larger than that of alginate/PVA or chitosan/PVA nanofibers without core-shell structure. On the other hand, both of alginate<sup>[18-19]</sup> and chitosan<sup>[20]</sup> have good absorption capacity. Obviously, water absorption capacity of alginate/PVA or chitosan/PVA nanofibers were lower to some extent. The loose and porous nanofibers film changed to the viscous and soft one following water absorption.

Wound healing is a fundamental response to tissue injuries. Healing involves overlapping steps of inflammation, cell migration and proliferation, neovascularization, extracellular matrix production and remodeling. An optimal wound dressing should facilitate healing. Nanofibers own very high specific surface area, leading to their high absorption capacity of water. The intense and soft film composed of nanofibers can protect the wounds from infection and over-drying. Moreover, the nanofibers film is ventilated and comfortable. The clean breeding condition of animals could make wound recover quickly. In the outdoor condition, the wound would be infected easily. If that, the antibacterial function of the coaxial nanofiber wound dressing become important. The antibacterial mechanism of the coaxial nanofibers should attribute to the interaction of the positively charged quaternary ammonium groups of chitosan and the negatively charged bacterial cell membranes, leading to loss of membrane permeability and leakage of intracellular components<sup>[21-22]</sup>. Modulation of pro-inflammatory factors (e.g., IL-6, TNF- $\alpha$ ) is important in wound healing. The levels of IL-6 and TNF- $\alpha$  increase sharply after burn. The nanofibers could make them nearly return to the normal levels after 21-days treatment. This may be due to the anti-inflammation effect of alginate<sup>[23]</sup> and anti-oxidation effect of chitosan<sup>[24]</sup>.

### 4 Conclusion

Chitosan has good antibacterial ability and alginate has strong water absorption capability. Furthermore, chitosan and alginate were combined together with the coaxially electrospinning technique to form the alginate/PVA/chitosan coaxial nanofibers. The nanofibers showed good water absorption capacity, antibacterial function, and improved wound healing effect. The coaxial nanofibers may directly or indirectly stimulate many factors, including

improvement of angiogenesis and vasculogenesis, inhibition of inflammatory factors, increase of fibroblast proliferations and collagen synthesis. These factors are important for proliferation of keratinocytes and fibroblasts, epithelialization, collagen synthesis, extracellular matrix remodeling and angiogenesis, leading to accelerated wound healing. The merits of chitosan and alginate are sufficiently demonstrated in the coaxial nanofibers. Therefore, alginate/PVA/chitosan coaxial nanofibers might be used as a novel wound dressing for treatment of deep partial-thickness burns.

## REFERENCES

- [1] MONSTREY S, HOEKSEMA H, VERBELEN J, et al. Assessment of burn depth and burn wound healing potential [J]. *Burns*, 2008, 34(6): 761-769.
- [2] CHEN B, YANG S, WU S. Progress in new carriers for topical medication of dermatology [J]. *Chin J Mod Appl Pharm(中国现代应用药学)*, 2018, 35(4): 615-621.
- [3] ZHU L, LIU X, DU L, et al. Preparation of asiaticoside-loaded coaxially electrospinning nanofibers and their effect on deep partial-thickness burn injury [J]. *Biomed Pharmacol*, 2016(83): 33-40.
- [4] SILL T J, RECUM H A V. Electrospinning: applications in drug delivery and tissue engineering [J]. *Biomaterials*, 2008, 29(13): 1989-2006.
- [5] KRSTIC M, RADOJEVIC M, STOJANOVIC D, et al. Formulation and characterization of nanofibers and films with carvedilol prepared by electrospinning and solution casting method [J]. *Eur J Pharm Sci*, 2017(101): 160-166.
- [6] CHENG L, SUN X, ZHAO X, et al. Surface biofunctional drug-loaded electrospun fibrous scaffolds for comprehensive repairing hypertrophic scars [J]. *Biomaterials*, 2016(83): 169-181.
- [7] JIANG H, HU Y, LI Y, et al. A facile technique to prepare biodegradable coaxial electrospun nanofibers for controlled release of bioactive agents [J]. *J Control Release*, 2005, 108(2/3): 237-243.
- [8] VYSLOUZILOVA L, BUZGO M, POKORNY P, et al. Needleless coaxial electrospinning: a novel approach to mass production of coaxial nanofibers [J]. *Int J Pharm*, 2017, 516(1/2): 293-300.
- [9] NASERI N, ALGAN C, JACOBS V, et al. Electrospun chitosan-based nanocomposite mats reinforced with chitin nanocrystals for wound dressing [J]. *Carbohydr Polym*, 2014(109): 7-15.
- [10] PEREIRA R F, CARVALHO A, GIL M H, et al. Influence of Aloe vera on water absorption and enzymatic *in vitro* degradation of alginate hydrogel films [J]. *Carbohydr Polym*, 2013, 98(1): 311-320.
- [11] DING Y, WANG B, YANG Y. Preparation of phenytoin sodium carboxymethyl chitosan microsphere and its bacteriostasis experiment research on periodontal common pathogenic bacteria [J]. *Chin J Mod Appl Pharm(中国现代应用药学)*, 2018, 35(4): 492-496.
- [12] HU D, WANG H, WANG L. Physical properties and antibacterial activity of quaternized chitosan/carboxymethyl cellulose blend films [J]. *Food Sci Tech*, 2016(65): 398-405.
- [13] UNNITHAN A R, GNANASEKARAN G, SATHISHKUMAR Y, et al. Electrospun antibacterial polyurethane-cellulose acetate-zein composite mats for wound dressing [J]. *Carbohydr Polym*, 2014(102): 884-892.
- [14] BONNINO C A, KREBS M D, SAQUING C D, et al. Electrospinning alginate-based nanofibers: from blends to crosslinked low molecular weight alginate-only systems [J]. *Carbohydr Polym*, 2011, 85(1): 111-119.
- [15] YANG Q, LI Z, HONG Y, et al. Influence of solvents on the formation of ultrathin uniform poly(vinyl pyrrolidone) nanofibers with electrospinning [J]. *J Polym Sci B*, 2004, 42(20): 3721-3726.
- [16] ZHOU Y, YANG H, LIU X, et al. Electrospinning of carboxyethyl chitosan/poly(vinyl alcohol)/silk fibroin nanoparticles for wound dressings [J]. *Int J Biol Macromol*, 2013(53): 88-92.
- [17] WANG X-Q, KRAVCHUK O, KIMBLE R M. A retrospective review of burn dressings on a porcine burn model [J]. *Burns*, 2010, 36(5): 680-687.
- [18] BANERJEE S, SINGH S, BHATTACHARYA S S, et al. Trivalent ion cross-linked pH sensitive alginate-methyl cellulose blend hydrogel beads from aqueous template [J]. *Int J Bio Macromol*, 2013(57): 297-307.
- [19] HRYNYK M, MARTINS-GREEN M, BARRON A E, et al. Alginate-PEG sponge architecture and role in the design of insulin release dressings [J]. *Biomacromolecules*, 2012, 13(5): 1478-1485.
- [20] AOYAGI S, ONISHI H, MACHIDA Y. Novel chitosan wound dressing loaded with minocycline for the treatment of severe burn wounds [J]. *Int J Pharm*, 2007, 330(1/2): 138-145.
- [21] CROISIER F, JEROME C. Chitosan-based biomaterials for tissue engineering [J]. *Eur Polym J*, 2013, 49(4): 780-792.
- [22] SARHAN W A, AZZAZY H M E. High concentration honey chitosan electrospun nanofibers: Biocompatibility and antibacterial effects [J]. *Carbohydr Polym*, 2015(122): 135-143.
- [23] MURAKAMI K, AOKI H, NAKAMURA S, et al. Hydrogel blends of chitin/chitosan, fucoidan and alginate as healing-impaired wound dressing [J]. *Biomaterials*, 2010, 31(1): 83-90.
- [24] CHEUNG R C F, NG T B, WONG J H, et al. Chitosan: an update on potential biomedical and pharmaceutical applications [J]. *Mar Drugs*, 2015, 13(8): 5156-5186.

收稿日期: 2018-10-24  
(本文责编: 蔡珊珊)